Research Article

Dynamic Characteristics of Amorphous Photovoltaic Module by Light-induced Degradation

Nitikorn Silsirivanich
Faculty of Architecture and Design, Rajamangala University of Technology Ruttanakosin, Nakhon Pathom, Thailand

Prungsak Auttaphut*
Department of Electrical Technology, Suan Sunandha Rajabhat University, Bangkok, Thailand

* Corresponding author. E-mail: prongsaku@gmail.com DOI: 10.14416/j.ijast.2018.08.002
Received: 14 March 2018; Accepted: 24 May 2018; Published online: 15 August 2018

Abstract
This paper is a study on the impacts of dynamic characteristics on the light-induced degradation phenomena, the modules under test were amorphous tandem (a-Si:H/a-Si:H). There dynamic characteristics of amorphous thin film silicon Photovoltaic module (PV module) by dynamic impedance technique. The *I-V* characteristics of Photovoltaic (PV) modules are generally measured at Standard Test Condition (STC) or in the dark. It's unable to explain the phenomena in the light-induced degradation in terms of material properties. Dynamic characteristics cannot be revealed by *I-V* curves measurements. Dynamic impedance were measured and analyzed by using the basic instrument. From the experimental results, it is found that dangling bonds and localized states phenomena resulting from light-induced degradation can obviously be reflected on dynamic parameter with forward biasing. In this paper show the PV module is stable stage about 148 kWh/m^2 or a month, The series resistance (R_S) is increased, shunt resistance (R_{sh}) and internal diode dynamic resistance ($R_d(V)$) are decreased continuously, Similarly, the diffusion capacitance ($C_D(V,\omega)$) were slightly decreased after light-induced by outdoor exposure. The decays observed can be proposed that there states localized of band tails are due to minority carrier lifetime an outside the transition region. It is proportional to the current of electricity, It is according to the Maximum current (I_m) and Maximum power (P_m) is decreasing by light-induced degradation.

Keywords: Amorphous silicon photovoltaic module, Dynamic characterization, Dynamic impedance, Light-induced degradation, *I-V* characteristic, Photovoltaic module

1 Introduction

Staebler and Wronski had reported that long exposure to light decreased the dark conductivity and photo conductivity of hydrogenated amorphous silicon material [1]–[5]. And this was reversed upon annealing at temperatures greater than 150°C for few hours. This is known as the "Staeble-Wronski Effect (SWE)".

The studies of dynamic characterization, they highlight solar cell impedances in terms of material properties [7]–[9], and measured solar cells under dark conditions with either forward bias or reversed bias conditions. This article describes dynamic impedance measurement and light-induced degradation study and explain $Z_{PV}(V, \omega)$ of a PV module from time and frequency domain analyses. The outline of this paper consists of theoretical static characteristic, background for $Z_{PV}(V, \omega)$ in frequency domain analysis and PV

Please cite this article as: N. Silsirivanich and P. Auttaphut, "Dynamic characteristics of amorphous photovoltaic module by light-induced degradation," *KMUTNB Int J Appl Sci Technol*, vol. 11, no. 4, pp. 273–277, Oct.–Dec. 2018.

module diagnostic method with $Z_{PV}(V, \omega)$. The detail of each section as following.

Static model of a solar cell or a PV module. A static characteristic of a solar cell or a PV module can be done by the measurement of current-voltage characteristic either under illumination (*I-V* curve) or in the dark (called dark *I-V* curve). In standard measurement, a static current-voltage characteristic or an *I-V* curve of a solar cell or a PV module is generally measured by using pulsed solar simulator according to IEC60904-9 standard and curve tracing with electronic load [6]. The parameters consist of open circuit voltage (V_{OC}), short circuit current (I_{SC}), voltage, current, and power at maximum power (V_m, I_m, and P_m), Fill Factor (*FF*), series resistance (R_s) and shunt resistance (R_{sh}). A series resistance (R_s) can be calculated from the slope of linear part near I_{SC}. A shunt resistance (R_{sh}) can be calculated from the slope of linear part near V_{OC}.

Dynamic characteristic description in the dark. The dynamic characteristic of a solar cells or a PV module can be derived from the dynamic impedance model or AC equivalent circuit [7]–[9]. The additional parameters, from static model, consist of a diffusion capacitance (C_D) and a junction or transient capacitance (C_T). The parallel capacitance (C_p) is resultant capacitance of C_D in parallel with C_T. The $C_T(V)$ is voltage dependent, and the $C_D(V, \omega)$ is voltage and frequency dependent. Figure 1 it shows the simplified dynamic impedance model. "The R_s and R_p can be determined by impedance loci plot at high frequency end and low frequency end interceptions on real part axis, respectively" [8], [9].

An AC impedance model of a solar cell or a PV module can be determined by an impedance spectroscopy method [7]–[9]. The measurement can be done in the dark with forward or reverse biasing. The closed-form equation of a solar cell dynamic impedance, $Z_{PV}(V, \omega)$, was derived and reported in our previous work [8], [9]. The AC-equivalent circuit of the solar cell including dynamic impedance as shown in Figure 1 can be modeled with a simplified equivalent circuit at the frequency ω consisting of one resistive component and one capacitive component in series in the form of $R_{PV}+jX_{PV}$ by the following [Equation (1)] [8].

$$Z_{PV} = R_{PV} + jX_{PV},$$

$$Z_{PV} = \left[R_s + \frac{R_p}{(\omega R_p C_p)^2 + 1} \right] - j \left[\frac{\omega R_p^2 C_p}{(\omega R_p C_p)^2 + 1} \right] \qquad (1)$$

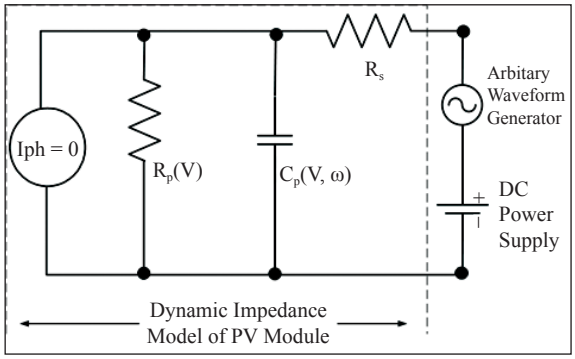

Figure 1: Simplify dynamic impedance model.

where R_{PV} – real part of dynamic impedance; X_{PV} – imaginary part of dynamic impedance; R_s–series resistance; R_p – parallel resistance – resultant resistance of shunt resistance R_{sh} in parallel with dynamic resistance of diode $R_d(V)$; $C_p(V, \omega)$ – parallel capacitance – resultant capacitance of transient capacitance $C_T(V)$ in parallel with diffusion capacitance $C_D(V, \omega)$; ω – signal frequency.

The R_s and R_p can be determined by impedance loci plot [8], [9] at a high-frequency end and low-frequency end interceptions on real part axis, respectively. AC equivalent circuit parameters can be determined by impedance loci plot. R_s and R_{sh} can be yielded by the interceptions on the real part axis. $R_d(V)$ can be calculated from R_p and R_{sh}. The diffusion capacitance $C_D(V, \omega)$ is dominant at forward bias condition. $C_T(V)$ is dominant at reverse bias condition.

2 Experimental

The measurements were made on a selected *a*-Si:H/*a*-Si:H tandem PV module consisting of 40 cells in series connection. The area of PV module is 0.78 m^2 (sized 0.65×1.20 m). The module structure is TCO/[*p*(*a*-SiO)/*i*(*a*-Si)/*n*(μc)/*p*(μc)/*i*(*a*-Si)/*n*(μc)]/Ag/Al.

The measurements is determined at three stages, before and after Natural sun light outdoor exposure test under maximum resistance load [6] for initial state (0 kWh/m^2), 35 kWh/m^2 and 148 kWh/m^2. The experiment consists of current-voltage characteristic measurements under dark and illumination condition, and the dynamic impedance measurement using dynamic impedance method.

Current-voltage characteristic measurement under illumination condition. *I-V* curves were measured by the Pasan Solar Simulator SS3B of the CES Solar Cells Testing Center (CSSC) of the University. The type of solar simulator is pulsed solar simulator according to IEC60904-9 standard [6]. The sweeping duration of electronic load curve tracing can be set in the range of 10 ms. The directions of curve tracing can be set from Short Circuit to Open Circuit (SCOC) direction. The measurements were done at standard test conditions: 1,000 W/m^2, Air- mass 1.5 and module temperature of 25°C by varying sweeping durations and curve tracing directions. To perform evaluation in standard method, the measurement is made under illumination at Standard Test Condition (STC) according to IEC61646 standard - clause 10.6 [6].

Current-voltage characteristic measurement under dark condition. *I-V* curves were measured by the Agilent 3498A data acquisition and Agilent N5769A DC power supply for bias voltage. The measurements were done in the dark at module temperature of 25°C with reverse bias voltages and forward bias voltages.

Dynamic impedance measurement in the dark. The experiments were fulfilled for measuring dynamic impedance of a PV module by using the method described in [8], [9]. The measurements were done in the dark at module temperature of 25°C with reverse bias voltages of 0.4 and 0.5 V/cells, and forward bias voltages of 0.4, 0.8 and 1.2 V/cells, respectively. The frequency range of modulating square wave signal was 10 Hz to 10 kHz with amplitude of about 10% of biasing voltage. The instrument consists of an Agilent 33250A arbitrary waveform generator, an audio frequency power amplifier, a Tektronix TDS 1002 digital oscilloscope, an Agilent 6032A DC power supply and a computer with data communication of instruments. The $Z_{PI}(V, \omega)$ can be calculated from the output responses by the MATLAB using the Fast Fourier Transform (FFT) analysis. The impedance loci were plotted and the essential parameters were calculated.

3 Results and Discussions

Current-voltage characteristic measurement under illumination condition. The *I-V* curves of light-induced degradation show as Figure 2 (a). There parameters measured results show as Table 1. Under illuminate condition, the measurements of *I-V* characteristics are use in most of standard measurements. The result of standard testing condition of initial state 0 kWh/m^2 to 148 kWh/m^2. R_S increases 6.7% by the contacts and bulk resistance, R_{sh} decreasing 16% with incerases leaked current of junction diode [1]–[3]. The I_m, P_m, and *FF* is decreases 3.75%, 3% and 0.7% respectively.

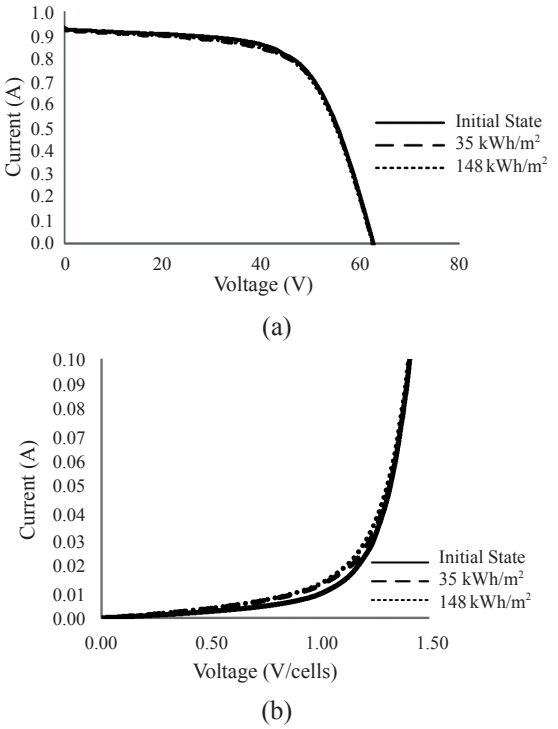

Figure 2: *I-V* curves at differential light-induced by outdoor durations is observed an under illuminate condition measurement (a) and dark condition measurement (b).

Table 1: STC measurement result at differential light-induced by outdoor durations is observed

Electric Parameter	Outdoor Exposures (kWh/m^2)		
	0 kWh/m^2	35 kWh/m^2	148 kWh/m^2
R_s, Ω	15	16	16
R_{sh}, Ω	1,022	860	853
V_m, V	47.0	47.0	47.0
V_{OC}, V	62.0	62.0	62.0
I_m, A	0.80	0.78	0.77
I_{SC}, A	0.92	0.92	0.92
P_m, W	37.6	36.6	36.2
η, %	4.6	4.6	4.6
FF, %	63.5	63.0	63.0

Under dark condition, the dark *I-V* curves of light-induced degradation show as Figure 2 (b). There results of Table 2, The interpretation results of dark *I-V* curves under the forward and reverse bias. The R_S is determined from the *I-V* curve when the diode is fully conducting. The R_{sh} is determined from the linear part of the *I-V* curves near the origin. The $R_d(_V)$ is determined from the *I-V* curves when the diode conducts to fully conduct. The $R_d(V)$ of the internal diode decrease 10% at the forward bias voltage. R_{sh} decreased 28% at the reverse bias voltage.

Table 2: Interpretations result of dark *I-V* curves of PV module

Outdoor Expossure (kWh/m^2)	R_S (Ω)	R_{sh} (kΩ)	R_d (Ω)
0 kWh/m^2	15	10.0	2.56
35 kWh/m^2	16	7.5	2.37
148 kWh/m^2	16	7.2	2.30

Dynamic impedance measurement in the dark. The dynamic characteristic of a PV module $Z_{PV}(V, \omega)$ can be described by the impedance loci plot and the derivation mentioned above. The dynamic impedance parameters of the AC equivalent circuit in Figure 1 can be calculated from the measurement in the dark with forward and reverse bias voltage. By dynamic impedance method [7]–[9], the voltage and frequency dependent parameter is diffusion capacitance (C_D). The voltage dependent parameters (C_T, R_s, R_d, and R_{sh}) can be revealed by impedance plot. It show R_s – series resistance; R_p – parallel resistance – resultant resistance of shunt resistance R_{sh} in parallel with dynamic resistance of diode $R_d(V)$ as Figure 3.

Parallel capacitance $C_p(V, \omega)$ as Figure 4. $C_p(V, \omega)$ – parallel capacitance–resultant capacitance of transient capacitance $C_T(V)$ in parallel with diffusion capacitance $C_D(V, \omega)$; ω – signal frequency. $C_T(V)$ is dominant at reverse bias condition and The diffusion capacitance $C_D(V, \omega)$ is dominant at forward bias condition.

In the dark with reverse bias. R_{sh} is dominant with low biasing voltage. It is due to $R_d(V)$ is much greater than R_{sh} because the diode is less conductive with reverse biasing. Therefore, $R_p(V)$ in Figure 3 is close to R_{sh}, It's decreased 12% with incerases leaked current of junction diode. $C_T(V)$ is more dominant than $C_D(V, \omega)$. Therefore, $C_T(V)$ is close to $C_p(V, \omega)$ as

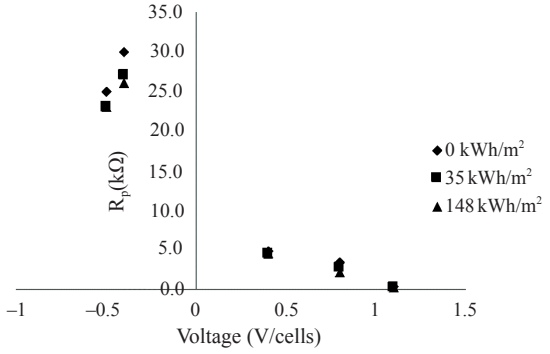

Figure 3: Parallel resistance $R_P(V)$ with reverse bias voltages and forward bias voltages.

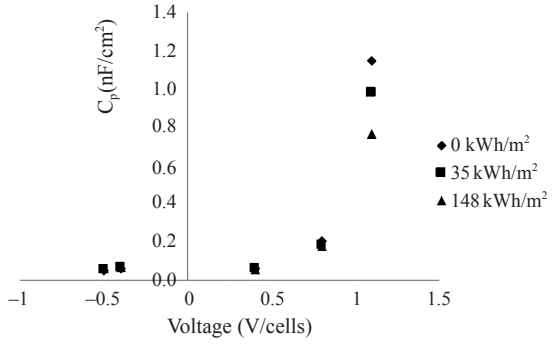

Figure 4: Parallel capacitance $C_p(V, \omega)$ plot with reverse bias voltages of 0.4 and 0.5 V/cells and forward bias voltages of 0.4, 0.8 and 1.2 V/cells.

shown in Figure 4. The *C-V* curves shown as $C_T(V)$ independent of light-induced degradation. It can be explained by basic formula which is obtained for parallel-plate capacitor (p-i, i-n junction) of area (square meter) and width of the depletion region (meter) containing a material of permittivity[1], [2].

In the dark with forward bias. $R_d(V)$ is dominant with forward biasing voltage because diode resistance normally decreases with increasing forward bias voltage. Therefore, $R_p(V)$ in Table 2 is close to R_d. $C_D(V, \omega)$ is more dominant than $C_T(V)$ with forward biasing. So, $C_D(V, \omega)$ it is shown in Figure 4. The *C-V* curves shown as $C_D(V, \omega)$ is maximum decreased 33% at near the diode conducts to fully conduct (1.2 V/cells). The decays of $C_D(V, \omega)$ due to defected of material outside the transition region by light-induced degradation. It's can be proposed for states localized of band tail, are due to

the increase in recombination rate and minority carrier lifetime is decreasing. It's defined as a rate of change of injected charge across a junction, is proportional to the current of electricity, It is correlating to the I_m and P_m the result of Table 1 is decreasing by light-induced degradation.

4 Conclusions

This work proposed the according to the dynamic impedance measurement technique in the dark condition and illumination measurement results (The *I-V* characteristics of Photovoltaic (PV) modules are generally measured at Standard Test Condition (STC)). It's unable to explain the phenomena in the light-induced degradation in terms of material properties. Dynamic characteristics cannot be revealed by *I-V* curves measurements. In this paper show the PV module is stable stage about 148 kWh/m^2 or a month, by P_m decreased less than 2% observation. In the dynamic impedance can be explained the light-induced degradation by dynamic parameters. The R_S is increased, R_{sh} and $R_d(V)$ are decreased continuously, Similarly, the $C_D(V, \omega)$ were slightly decreased after light-induced by outdoor exposure. The decays of $C_D(V, \omega)$ observed, It's pave the way for proposed that there states localized of band tails are due to minority carrier lifetime outside the transition region [1]–[3], [7]. It's can be presented the increase in recombination rate. It's defined as rate of change of injected charge across a junction, is proportional to produce electricity with PV modules.

Acknowledgments

The authors wish to acknowledge great supports from CSSC, RMUTR and SSRU for providing excellent research facilities, and valuable advices given by Dr. Dhyrayut Chenvidhya.

References

[1] A. Luque and S. Hegedus, *Handbook of Photovoltaic Science and Engineering*. New Jersey: John Wiley & Sons, Ltd., 2003, pp. 505–565.

[2] Y. Hamakawa, *Amorphous Semiconductor Technology & Devices*. Netherlands: North-Holland Publishing Co., 1982, pp. 33–199.

[3] R. F. Pierret, *Semiconductor Device Fundamentals. Boston*, Massachusetts: Addison-Wesley Publishing Company, Inc., 1996, pp. 23–344.

[4] B. Pivaca, I. Kovacevica, and I. Zulim, "Defects induced in amorphous silicon thin films by light soaking," *Thin Solid Films*, vol. 403–404, pp. 513–516, 2002.

[5] G. Nobile and M. Morana, "Light soaking effect in a-Si:H based n-i-p and p-i-n solar cell," *Solar Energy Materials and Solar Cells*, vol. 76 , pp. 511–520, 2003.

[6] The International Electrotechnical Commission (IEC), *Thin-Film Terrestrial Photovoltaic (PV) Modules - Design qualification and type approval*, 2nd ed., Switzerland: IEC publications, 2008, pp. 21–22.

[7] R. Ani Kumar, M. S. Suresh, and J. Nagaraju, "Effect of solar array capacitance on the performance of switching shunt voltage regulator," *IEEE Transection Power Electrics*, vol. 21, no. 2, pp. 543–548, 2006.

[8] D. Chenvidhya, K. Kirtikara, and C. Jivacate, "PV module dynamic impedance and its voltage and frequency dependencies," *Solar Energy Materials and Solar Cells*, vol. 86, pp. 243–251, 2005.

[9] N. Silsirivanich, D. Chenvidhya, K. Kirtikara, K. Sriprapha, J. Sritharathikhun, R. Songprakorp, and C. Jivacate, "Non stationary effects at photovoltaic module characterization using pulsed solar simulator," *Journal of Apply Spectroscopy*, vol. 82, no. 2, pp. 293–292, 2015.